



# Clinical implementation of accelerated T<sub>2</sub> mapping: Quantitative magnetic resonance imaging as a biomarker for annular tear and lumbar disc herniation

Marcus Raudner<sup>1,2</sup> · Markus M. Schreiner<sup>3</sup> · Tom Hilbert<sup>4,5,6</sup> · Tobias Kober<sup>4,5,6</sup> · Michael Weber<sup>1</sup> · Anna Szelényi<sup>1</sup> · Reinhard Windhager<sup>3</sup> · Vladimir Juras<sup>2,7</sup> · Siegfried Trattnig<sup>1,2</sup>

Received: 12 June 2020 / Revised: 20 October 2020 / Accepted: 17 November 2020 / Published online: 3 December 2020  
© The Author(s) 2020

## Abstract

**Objectives** This study evaluates GRAPPATINI, an accelerated T<sub>2</sub> mapping sequence combining undersampling and model-based reconstruction to facilitate the clinical implementation of T<sub>2</sub> mapping of the lumbar intervertebral disc.

**Methods** Fifty-eight individuals (26 females, 32 males, age 23.3 ± 8.0 years) were prospectively examined at 3 T. This cohort study consisted of 19 patients, 20 rowers, and 19 volunteers. GRAPPATINI was conducted with the same parameters as a conventional 2D multi-echo spin-echo (MESE) sequence in 02:27 min instead of 13:18 min. Additional T<sub>2</sub> maps were calculated after discarding the first echo (T<sub>2-WO1ST</sub>) and only using even echoes (T<sub>2-EVEN</sub>). Segmentation was done on the four most central slices. The resulting T<sub>2</sub> values were compared for all four measurements.

**Results** T<sub>2-GRAPPATINI</sub>, T<sub>2-MESE</sub>, T<sub>2-EVEN</sub>, and T<sub>2-WO1ST</sub> of the nucleus pulposus of normal discs differed significantly from those of bulging discs or herniated discs (all  $p < 0.001$ ). For the posterior annular region, only T<sub>2-GRAPPATINI</sub> showed a significant difference ( $p = 0.011$ ) between normal and herniated discs. There was a significant difference between T<sub>2-GRAPPATINI</sub>, T<sub>2-MESE</sub>, T<sub>2-EVEN</sub>, and T<sub>2-WO1ST</sub> of discs with and without an annular tear for the nucleus pulposus (all  $p < 0.001$ ). The nucleus pulposus' T<sub>2</sub> at different degeneration states showed significant differences between all group comparisons of Pfirrmann grades for T<sub>2-GRAPPATINI</sub> ( $p = 0.000–0.018$ ), T<sub>2-MESE</sub> ( $p = 0.000–0.015$ ), T<sub>2-EVEN</sub> ( $p = 0.000–0.019$ ), and T<sub>2-WO1ST</sub> ( $p = 0.000–0.015$ ).

**Conclusions** GRAPPATINI facilitates the use of T<sub>2</sub> values as quantitative imaging biomarkers to detect disc pathologies such as degeneration, lumbar disc herniation, and annular tears while simultaneously shortening the acquisition time from 13:18 to 2:27 min.

## Key Points

- T<sub>2-GRAPPATINI</sub>, T<sub>2-MESE</sub>, T<sub>2-EVEN</sub>, and T<sub>2-WO1ST</sub> of the nucleus pulposus of normal discs differed significantly from those of discs with bulging or herniation (all  $p < 0.001$ ).
- The investigated T<sub>2</sub> mapping techniques differed significantly in discs with and without annular tearing (all  $p < 0.001$ ).

**Summary statement** GRAPPATINI facilitates T<sub>2</sub> mapping as a quantitative imaging biomarker that can be used for the quantitative assessment of the nucleus pulposus, which correlates with degeneration and lumbar disc herniation and may be associated with annular tears, while shortening the acquisition time from 13:18 to 2:27 min.

✉ Siegfried Trattnig  
siegfried.trattnig@akhwien.at

<sup>1</sup> Department of Biomedical Imaging and Image-guided Therapy, High Field MR Center, Medical University of Vienna, Lazarettgasse 14, 1090 Vienna, Austria

<sup>2</sup> Christian Doppler Laboratory for Clinical Molecular MR Imaging (MOLIMA), Department of Biomedical Imaging and Image-guided Therapy, High Field MR Center, Medical University of Vienna, Vienna, Austria

<sup>3</sup> Department of Orthopaedics and Trauma Surgery, Medical University of Vienna, Vienna, Austria

<sup>4</sup> Advanced Clinical Imaging Technology, Siemens Healthcare, Lausanne, Switzerland

<sup>5</sup> Department of Radiology, Lausanne University Hospital and University of Lausanne, Lausanne, Switzerland

<sup>6</sup> LTS5, Ecole Polytechnique Fédérale de Lausanne (EPFL), Lausanne, Switzerland

<sup>7</sup> Department of Imaging Methods, Institute of Measurement Science, Bratislava, Slovakia

- *The nucleus pulposus'  $T_2$  showed significant differences between different stages of degeneration in all group comparisons for  $T_2$ -GRAPPATINI ( $p = 0.000$ – $0.018$ ),  $T_2$ -MESE ( $p = 0.000$ – $0.015$ ),  $T_2$ -EVEN ( $p = 0.000$ – $0.019$ ), and  $T_2$ -WO1ST ( $p = 0.000$ – $0.015$ ).*

**Keywords** Spine · Intervertebral disc · Intervertebral disc displacement · Intervertebral disc degeneration

## Abbreviations

2D-MESE	Two-dimensional multi-echo spin-echo sequence
3D-TESS	Three-dimensional triple-echo steady-state sequence
CI95	95% confidence interval
CPMG	Carr-Purcell-Meiboom-Gill sequence
ERL	Echo train length
EVEN	Reconstructed $T_2$ maps based on MESE data based on only even echoes
GRAPPA	Generalized autocalibrating partial parallel acquisition
GRAPPATINI	Sequence combining MARTINI and GRAPPA
MARTINI	Model-based accelerated relaxometry by iterative non-linear inversion
MRF	Magnetic resonance fingerprinting
qMRI	Quantitative magnetic resonance imaging
SAR	Specific absorption rate
SD	Standard deviation
TE	Time to echo (in milliseconds)
TR	Time to repetition (in ms if not otherwise stated)
WO1ST	Reconstructed $T_2$ maps based on MESE data excluding the first echo

## Introduction

Lower back pain (LBP) still ranks as the most common cause for years lived with disability (YLD) and disability-adjusted life years (DALY) according to the Global Burden of Disease Studies of 2016 [1].

The intervertebral disc (IVD) is mainly composed of an inherent architecture of dense collagen fibers, the annulus fibrosus, surrounding the nucleus pulposus with its high concentration of glycosaminoglycans (GAG) that facilitate its water-storing capabilities [2].

Degenerative disc disease, caused by an irreversible decay of the IVD structural integrity, leads to an inadequate biomechanical response to pressure or load [3]. This puts patients at risk for disc herniation, annular tear, or osteochondrosis and leads to chronic pain which is further aggravated by the visceral pain qualities of chronic lower back pain caused by the sinuvertebral nerve endings that sprout into the disc [4].

Visceral pain aggravates with distension and is highly responsive to inflammatory stimuli. It is difficult to localize, while the pain is often described as profound, pressing, and blunt.

To assess the intervertebral disc, non-invasive MRI established itself as the method of choice [5].

Using conventional magnetic resonance imaging (MRI), intervertebral disc degeneration is typically scored using the Pfirrmann classification [6].

However, this presumably simple task is only semi-quantitative, depends on weighted contrast images, is evaluator-dependent, and comes with pitfalls such as magnetization transfer effects, which can cause a lower signal intensity in the nucleus pulposus, resulting in a lower signal intensity and therefore a lower Pfirrmann classification.

Quantitative magnetic resonance imaging (qMRI) methods such as  $T_2$  mapping provide objective results, which have already shown excellent discriminability when it comes to disc degeneration [7].

As  $T_2$  mapping is widely available and well-suited for the evaluation of the disc's biochemical state, correlating with histology, water content, and degeneration is one of the most often used quantitative methods in research regarding low back pain [8].

Also,  $T_2$  mapping can depict changes in very early stages of disc degeneration that remain invisible to conventional morphological imaging sequences [9].

$T_2$  mapping of the IVD can therefore be considered an important biomarker in clinical applications [10, 11].

Conventional  $T_2$  mapping is usually performed using a two-dimensional multi-echo spin-echo (2D-MESE) sequence which samples multiple contrasts at successive, equally spaced echo times (TE) [12]. The resulting  $T_2$  maps are reconstructed by performing a mono-exponential voxel-wise fit on the measured signal decay. However, the clinical feasibility of the MESE sequence is limited due to long acquisition times and specific absorption rate (SAR) limitations. These limitations become especially restrictive at a higher in-plane resolution (e.g.,  $1 \times 1 \text{ mm}^2$ ) [13].

To overcome these obstacles, GRAPPATINI combines “model-based accelerated relaxometry by iterative non-linear inversion” (MARTINI) and “generalized autocalibrating partial parallel acquisition” (GRAPPA) [14]. GRAPPATINI uses Cartesian sampling with an undersampling pattern organized in blocks based on the chosen undersampling factor. Also, GRAPPA is used for further acceleration by sampling only every other phase-encoding step within a block. The fitting, which

is integrated in the image reconstruction, discards the first echo as it is commonly done for MESE data. GRAPPATINI has been successfully applied in other studies with continuously robust  $T_2$  values compared to a typical MESE sequence in MRI of the brain, knee, prostate, and liver [14].

The aim of this study was (a) to investigate whether GRAPPATINI can be used in direct comparison with  $T_2$  maps reconstructed from a conventional MESE sequence dataset, (b) to discriminate between different degeneration states, reflected by Pfirrmann classifications, (c) to differentiate discs with and without herniation, and (d) to distinguish between discs with and without annular tear.

## Methods and materials

### Patients and study design

Upon approval by the institutional review board, 60 individuals were prospectively enrolled in this prospective cohort study. Initially, 20 patients, 20 healthy volunteers, and 20 professional rowers were registered between January 2017 and November 2018. The rowers were included in the study to assess early degenerative changes. One patient aborted the measurement due to pain in prolonged supine position and one healthy volunteer was excluded due to motion artifacts in all sequences. In total, 58 MRIs were evaluated (26 females, 32 males, mean age  $23.3 \pm 8.1$  years; ranging from 16 to 50 years) from 19 patients (9 females, 10 males, mean age  $28.3 \pm 7.5$  years, ranging from 19 to 49 years), 19 volunteers (9 females, 10 males, mean age  $21.5 \pm 7.3$  years, ranging from 17 to 50 years), and 20 rowers (8 females, 12 males, mean age  $20.3 \pm 7.5$  years, ranging from 16 to 50 years). No measurement of the remaining 58 analyzed individuals had to be excluded due to artifacts or other measurement-specific reasons.

Inclusion criteria were 16 to 90 years of age, more than two exercises longer than 1 h per week (rowers only), more than 18 months of training (rowers only), or persistent low back pain (patients only). Exclusion criteria were previous spine surgery, a scoliosis with a Cobb angle of more than  $15^\circ$ , a present oncological diagnosis, a systemic disease affecting bone or cartilage, and claustrophobia.

The study population was chosen specifically to compare young individuals with different degrees of spinal load during everyday life to assess early degenerative changes alongside comparably healthy discs in order to cover a wide spectrum of intervertebral disc states. This rationale seemed adequate to assess the broad applicability of different  $T_2$  mapping techniques as the results should be comparable in healthy, degenerated, or herniated discs or discs with annular tears as the resulting  $T_2$  values can be quite different depending on the discs state.

### MRI

MR examinations were performed at a field strength of 3 T (MAGNETOM Prisma<sup>fit</sup>, Siemens Healthcare) with a gradient strength of 80 mT/m, using a 32-channel spine matrix coil in supine position. Individuals received a standard leg support with a maximum height of 15 cm placed under their knees during the measurement. The protocol consisted of the following morphological sequences: sagittal  $T_1$ -weighted TSE, sagittal  $T_2$ -weighted TSE, sagittal  $T_2$ -weighted STIR, and a coronal and axial  $T_2$ -weighted TSE sequence with three sections per intervertebral disc. After the morphological sequences,  $T_2$  mapping was performed with a MESE sequence and the GRAPPATINI prototype directly afterwards.

A repetition time (TR) of 3500 ms ( $\geq 3 \times T_1$ , estimated at  $\approx 1000$  ms) was used in the  $T_2$  mapping sequences to recover the magnetization in every voxel prior to every echo train [14, 15].

A known caveat in  $T_2$  mapping is the signal component that arises from stimulated echoes. These are additional signal components which result in an increased and oscillating signal intensity starting from the second echo. Stimulated echoes are caused by suboptimal refocusing pulse angles due to  $B_1$  field inhomogeneity and imperfect slice profiles. Well-known ways to assure a good and stable fitting in spite of these wrong signal components are either to discard the first echo or to use only even echoes for the  $T_2$  map reconstruction [16].

Therefore, the echoes acquired with the MESE sequence were used to calculate two additional  $T_2$  maps directly on the scanner using MapIT (Siemens Healthcare) without the first echo (WO1ST) and using only even echoes (EVEN).

GRAPPATINI was set to an undersampling factor of 5 and two-fold GRAPPA, effectively resulting in ten-fold undersampled k-space data relative to a fully sampled acquisition for the  $T_2$  map reconstruction. The reference MESE sequence used only a conventional two-fold GRAPPA acceleration. GRAPPATINI  $T_2$  maps were automatically reconstructed as previously reported [14].

The sequence parameters for all morphological and  $T_2$  mapping sequences are listed in Table 1.

### Image analysis

Morphological images were assessed strictly adhering to the Lumbar Disc Nomenclature 2.0 of Fardon et al [17]. Additionally, all discs were scored after Pfirrmann et al [6].

The resulting images were manually segmented on the sagittal  $T_2$ -weighted TSE sequence using the four most central slices by a radiology resident with 5 years of experience in musculoskeletal imaging using ITK-Snap [18]. First, a strict geometrical order was followed labeling the anterior and posterior 20% as annulus fibrosus with the central 60% of the diameter representing the nucleus pulposus. This was then

**Table 1** Sequence parameters

Parameter	T <sub>2</sub> w TSE	GRAPPATINI	Multi-echo Spin echo
Plane	Sagittal	Sagittal	Sagittal
No. of slices	8	8	8
Slice thickness (mm)	4	4	4
Interslice gap (mm)	0.4 mm	0.4 mm	0.4
Field of view (mm <sup>2</sup> )	260 × 260	260 × 260	260 × 260
Acquisition matrix	384 × 230	378 × 227	384 × 230
Voxel size (mm <sup>3</sup> )	0.7 × 0.7 × 4	0.7 × 0.7 × 4	0.7 × 0.7 × 4
Phase encoding direction	A >> P	A >> P	A >> P
Time to repetition (TR in ms)	3500	3500	3500
Time to echo (TE in ms)	99	9 to 144 ms 16 echoes	9 to 144 ms 16 echoes
No. of averages	1	1	1
GRAPPA	2	2	2
Undersampling factor	–	5	–
Flip angle	160°	180°	180°
Bandwidth (Hz/Px)	224	224	224
Acquisition time	02:01	02:27	13:18

manually refined depending on the individual discs. An example is depicted in Fig. 1. Individual labels for each discs' ventral and posterior annular region and the nucleus pulposus of every of the five lumbar discs were drawn. Using Elastix [19], the segmentation was then copied over to the T<sub>2</sub> maps after successful automatic co-registration.

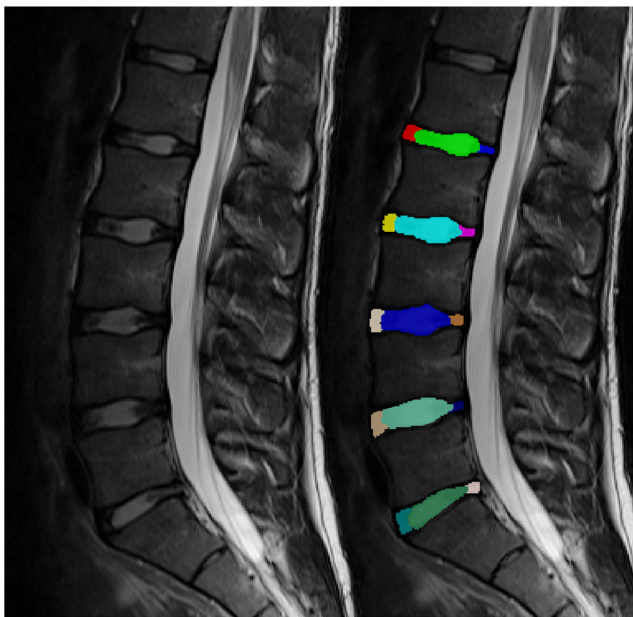


**Fig. 1** Sagittal T<sub>2</sub>-weighted contrast (left) with a color-coded overlay visualizing the segmentation done in ITK-SNAP (right). Every intervertebral disc was segmented in three individual regions of interest (ROIs): ventral annulus fibrosus, nucleus pulposus, and posterior annulus fibrosus. This case shows an annular tear in L5/S1

## Statistical evaluation

All statistical analyses were performed by a biomedical statistician using IBM SPSS for Windows version 25 (IBM). Given metric and normal distributed data are described using mean ± standard deviation (SD). In case of skewed metric data, median (95% confidence intervals) was used. Correlations were assessed using Spearman's correlation coefficient. Univariate ANOVA with post hoc tests depending on homogeneity of variances choosing either GT2 after Hochberg (no difference in variance) or Games-Howell (different variance) were used to compare groups (e.g., according to Pfirrmann grading). ROC analyses were used to test for discriminability regarding disc herniation, bulging, and annular tear.

A *p* value of ≤ 0.05 was considered to indicate statistically significant results. In order to avoid an increasing error of the second type, no multiplicity corrections were performed [20].

## Results

### T<sub>2</sub> mapping methods—GRAPPATINI and conventional MESE

Overall, the nucleus pulposus T<sub>2-GRAPPATINI</sub> (91.8 ms; CI95 89.2–94.5) showed a very strong Spearman correlation coefficient (all *p* < 0.001; *r* = 0.919 to 0.926) when compared with

$T_{2\text{-MESE}}$  (104.7 ms; CI95 101.3–108.1) as well as with  $T_{2\text{-EVEN}}$  (93.3 ms; CI95 90.5–96.2) and  $T_{2\text{-WO1ST}}$  (94.1 ms; CI95 91.2–97.0). Overall,  $T_{2\text{-MESE}}$  showed significantly higher  $T_2$  values in the nucleus pulposus than  $T_{2\text{-GRAPPATINI}}$ ,  $T_{2\text{-WO1ST}}$ , and  $T_{2\text{-EVEN}}$  (all  $p < 0.001$ ).

The posterior annulus fibrosus assessment showed a fair Spearman correlation (all  $p < 0.001$ ;  $r = 0.446$  to  $0.465$ ) of  $T_{2\text{-GRAPPATINI}}$  (47.7 ms; CI95 46.8–48.5),  $T_{2\text{-MESE}}$  (46.6 ms; CI95 45.4–47.8),  $T_{2\text{-EVEN}}$  (43.4 ms; CI95 42.2–44.5), and  $T_{2\text{-WO1ST}}$  (44.8 ms; 95CI 43.5–46.0).

Overall,  $T_{2\text{-MESE}}$  showed significantly higher  $T_2$  values in the posterior annular region than  $T_{2\text{-WO1ST}}$  and  $T_{2\text{-EVEN}}$  (both  $p < 0.001$ ). However,  $T_{2\text{-MESE}}$  showed insignificantly lower  $T_2$  compared to  $T_{2\text{-GRAPPATINI}}$  ( $p = 0.074$ ).

For an overview of all the different assessments and the resulting average median  $T_2$  values with 95% confidence intervals, see Table 2.

### Lumbar disc herniation assessment

Of all evaluated 290 intervertebral discs, 46 were labeled as bulging discs in 29 individuals and 40 showed lumbar disc herniation in 25 individuals.

$T_{2\text{-GRAPPATINI}}$ ,  $T_{2\text{-MESE}}$ ,  $T_{2\text{-EVEN}}$ , and  $T_{2\text{-WO1ST}}$  of the nucleus pulposus of normal discs differed significantly from those of bulging discs or herniated discs ( $p < 0.001$ ). There was no significant difference between bulging discs or herniated discs for  $T_{2\text{-GRAPPATINI}}$  ( $p = 0.682$ ),  $T_{2\text{-MESE}}$  ( $p = 0.072$ ),  $T_{2\text{-EVEN}}$  ( $p = 0.076$ ), or  $T_{2\text{-WO1ST}}$  ( $p = 0.075$ ).

For the posterior annular region, only  $T_{2\text{-GRAPPATINI}}$  showed a significant difference ( $p = 0.011$ ) between normal and herniated discs. All other group comparisons of  $T_{2\text{-GRAPPATINI}}$ ,  $T_{2\text{-MESE}}$ ,  $T_{2\text{-EVEN}}$ , and  $T_{2\text{-WO1ST}}$  showed non-significant results ( $p = 0.086$  to  $0.999$ ). An example of a patient with herniation in segment L5/S1 is given in Fig. 2 with color-coded  $T_2$  map overlays.

Calculating a receiver operating characteristic (ROC) assessing healthy discs with neither herniation nor bulging present using the NP  $T_2$ , the area under the curve (AUC) was 0.895 (0.851–0.939) for  $T_{2\text{-GRAPPATINI}}$ , 0.888 (0.844–0.931) for  $T_{2\text{-MESE}}$ , 0.888 (0.844–0.931) for  $T_{2\text{-EVEN}}$ , and 0.890 (0.847–0.933) for  $T_{2\text{-WO1ST}}$ .

Calculating an ROC for bulging discs, the AUC was 0.810 (0.742–0.878) for  $T_{2\text{-GRAPPATINI}}$ , 0.774 (0.700–0.849) for  $T_{2\text{-MESE}}$ , 0.775 (0.700–0.849) for  $T_{2\text{-EVEN}}$ , and 0.776 (0.702–0.850) for  $T_{2\text{-WO1ST}}$ .

Calculating a receiver operating characteristic (ROC) assessing disc herniation using the NP  $T_2$ , the area under the curve (AUC) was 0.845 (0.787–0.904) for  $T_{2\text{-GRAPPATINI}}$ , 0.872 (0.829–0.916) for median  $T_{2\text{-MESE}}$ , 0.872 (0.829–0.915) for median  $T_{2\text{-EVEN}}$ , and 0.874 (0.831–0.917) for median  $T_{2\text{-WO1ST}}$ .

### High-intensity zone and annular tear assessment

Of all 290 intervertebral discs assessed, 32 showed a high-intensity zone in 22 individuals in the posterior annular region, indicating annular tearing.

There was a significant difference between  $T_{2\text{-GRAPPATINI}}$ ,  $T_{2\text{-MESE}}$ ,  $T_{2\text{-EVEN}}$ , and  $T_{2\text{-WO1ST}}$  of discs with and without HIZ for both the nucleus pulposus and the posterior annular region (all  $p < 0.001$ ).

There was one exception with the posterior annular region closely missing the level of significance in the  $T_{2\text{-GRAPPATINI}}$  assessment ( $p = 0.052$ ).

Calculating an ROC for HIZ for the nucleus pulposus  $T_2$ , the AUC was 0.919 (0.886–0.953) for  $T_{2\text{-GRAPPATINI}}$ , 0.913 (0.873–0.953) for  $T_{2\text{-MESE}}$ , 0.911 (0.871–0.950) for  $T_{2\text{-EVEN}}$ , and 0.915 (0.876–0.954) for  $T_{2\text{-WO1ST}}$ . An example patient with a combination of lumbar disc herniation and annular tear of the L5/S1 segment alongside a HIZ in the L4/L5 segment is given in Fig. 3 with color-coded  $T_2$  map overlays.

### $T_2$ value differences for respective Pfirrmann grades

Of all 290 discs, the Pfirrmann grades were distributed as follows: I, 151 IVDs; II, 55 IVDs; III, 35 IVDs; IV, 48 IVDs; and V, 1.

For the NP, there was a significant difference between all group comparisons of Pfirrmann grades for  $T_{2\text{-GRAPPATINI}}$  ( $p$  value 0.000 to 0.018),  $T_{2\text{-MESE}}$  (0.000 to 0.015),  $T_{2\text{-EVEN}}$  (0.000 to 0.019), and  $T_{2\text{-WO1ST}}$  (0.000 to 0.015).

The annular region showed less discriminability between Pfirrmann grades for  $T_{2\text{-GRAPPATINI}}$  ( $p$  value 0.027 to 0.991),  $T_{2\text{-MESE}}$  (0.000 to 0.979),  $T_{2\text{-EVEN}}$  (0.002 to 0.995), and  $T_{2\text{-WO1ST}}$  (0.005 to 1.000).

### Discussion

Our data show that GRAPPATINI is capable of significantly shortening the acquisition time needed for accurate  $T_2$  mapping from 13:18 to 2:27 min while maintaining the known advantages of quantitatively reflecting the most common disc pathologies.

$T_{2\text{-GRAPPATINI}}$  of the nucleus pulposus showed an AUC comparable to the other methods when assessing discs with neither bulging nor herniation present. The same was true when assessing discs for bulging. Additionally,  $T_{2\text{-GRAPPATINI}}$  showed the only significant difference in the posterior annular region for healthy discs compared to discs with herniation present. Furthermore,  $T_{2\text{-GRAPPATINI}}$  showed an AUC equally high as the other methods for HIZ present in the annulus fibrosus.

Over a decade ago, it has already been demonstrated by Perry et al and Watanabe et al that  $T_2$  mapping may be

**Table 2** T<sub>2</sub> values for each assessment with 95% confidence intervals

Comparison of T <sub>2</sub> relaxation time measurements				
	T <sub>2</sub> -GRAPPATINI (CI95)	T <sub>2</sub> -MESE (CI95)	T <sub>2</sub> -EVEN (CI95)	T <sub>2</sub> -WO1ST (CI95)
<b>Lumbar disc herniation</b>				
Nucleus pulposus				
Normal ( <i>n</i> = 204)	101.3 (98.8–103.7)	116.1 (112.6–119.6)	103.1 (100.3–106.0)	104.0 (101.2–106.9)
Bulging ( <i>n</i> = 46)	70.9 (64.9–76.9)	81.7 (74.5–88.9)	73.6 (67.4–79.9)	74.2 (67.9–80.4)
Herniation ( <i>n</i> = 40)	67.8 (63.3–72.3)	72.8 (69.2–76.4)	65.9 (62.7–69.1)	66.4 (63.2–69.6)
Mean ( <i>n</i> = 290)	91.8 (89.2–94.5)	104.7 (101.3–108.1)	93.3 (90.5–96.2)	94.1 (91.2–97.0)
Annulus fibrosus				
Normal ( <i>n</i> = 204)	47.0 (46.0–48.0)	45.6 (44.1–47.1)	42.5 (41.0–43.9)	43.9 (42.3–45.5)
Bulging ( <i>n</i> = 46)	48.1 (45.8–50.4)	48.6 (46.1–51.0)	45.4 (43.1–47.6)	47.0 (44.6–49.5)
Herniation ( <i>n</i> = 40)	50.7 (48.4–53.1)	49.5 (46.0–53.0)	45.6 (42.5–48.7)	46.7 (43.4–50.0)
Mean ( <i>n</i> = 290)	47.7 (46.8–48.5)	46.6 (45.4–47.8)	43.4 (42.2–44.5)	44.8 (43.5–46.0)
<b>Annular tear</b>				
Nucleus pulposus				
No tear ( <i>n</i> = 258)	95.6 (93.1–98.2)	109.2 (105.8–112.6)	97.2 (94.3–100.1)	98.1 (95.2–100.9)
Tear ( <i>n</i> = 32)	61.0 (57.7–64.3)	68.3 (64.3–72.3)	62.0 (58.5–65.6)	62.3 (58.8–65.9)
Mean ( <i>n</i> = 290)	91.8 (89.2–94.5)	104.7 (101.3–108.1)	93.3 (90.5–96.2)	94.1 (91.2–97.0)
Annulus fibrosus				
No tear ( <i>n</i> = 258)	47.4 (46.4–48.3)	45.8 (44.4–46.9)	42.5 (41.3–43.7)	43.9 (42.6–45.2)
Tear ( <i>n</i> = 32)	50.1 (48.0–52.2)	54.2 (50.2–58.2)	50.4 (46.8–54.0)	51.8 (48.0–55.6)
Mean ( <i>n</i> = 290)	47.7 (46.8–48.5)	46.6 (45.4–47.8)	43.4 (42.2–44.5)	44.8 (43.5–46.0)
<b>Pfirmann classification</b>				
Nucleus pulposus				
I ( <i>n</i> = 151)	104.7 (102.1–107.3)	120.4 (116.5–124.3)	106.8 (103.6–109.9)	107.8 (104.6–110.9)
II ( <i>n</i> = 55)	97.1 (92.8–101.5)	109.9 (104.3–115.5)	98.4 (93.8–103.1)	99.1 (94.4–103.8)
III ( <i>n</i> = 35)	73.0 (68.7–77.3)	81.2 (75.8–86.6)	73.3 (68.8–77.9)	73.8 (69.3–78.3)
IV ( <i>n</i> = 48)	59.7 (57.5–61.8)	67.2 (64.8–69.7)	60.5 (58.4–62.6)	61.1 (59.0–63.2)
V ( <i>n</i> = 1)	58.3	61.0	53.5	55.0
Annulus fibrosus				
I ( <i>n</i> = 151)	46.7 (45.5–47.9)	44.6 (43.1–46.2)	41.7 (40.1–43.3)	43.0 (41.3–44.7)
II ( <i>n</i> = 55)	47.4 (45.1–49.8)	46.7 (43.5–49.8)	43.5 (40.5–46.6)	45.5 (42.0–49.0)
III ( <i>n</i> = 35)	48.7 (46.5–51.0)	48.2 (45.6–50.9)	44.7 (42.3–47.1)	45.6 (43.2–48.1)
IV ( <i>n</i> = 49)	50.2 (48.2–52.2)	51.7 (48.3–55.0)	47.6 (44.7–50.4)	49.0 (46.0–51.9)
V ( <i>n</i> = 0)	47.0	43.5	39.0	39.5

employed to assess the ultrastructural composition of intervertebral discs, namely highly hydrated glycosaminoglycans (GAG) in the nucleus pulposus and dense collagen fibers in the area of the annulus fibrosus [9, 21].

With ongoing degeneration, the IVD GAG content decreases, leading to a falling swelling pressure and an increased risk for annular tears and disc herniation [2, 22].

Since allegedly simple tasks, such as the semiquantitative Pfirmann classification [6] for degeneration assessment, can also be prone to error due to magnetization transfer effects or observer bias, quantitative data are desirable to obtain more objective results. T<sub>2</sub> mapping can do

that with similar or better discriminability when it comes to disc degeneration [7, 23].

In line with this statement, Schultz et al reported that the biomechanical properties of the intervertebral discs are better correlated with the collagen fiber structure integrity than with the Pfirmann classification [24]. Also, Marinelli et al showed that T<sub>2</sub> mapping correlated with the water and proteoglycan content of the nucleus pulposus in a histological specimen study of calf and human discs [11].

Ogon et al even showed significant differences in the posterior annular region with lower T<sub>2</sub> values in patients with chronic lower back pain compared to healthy controls [8].

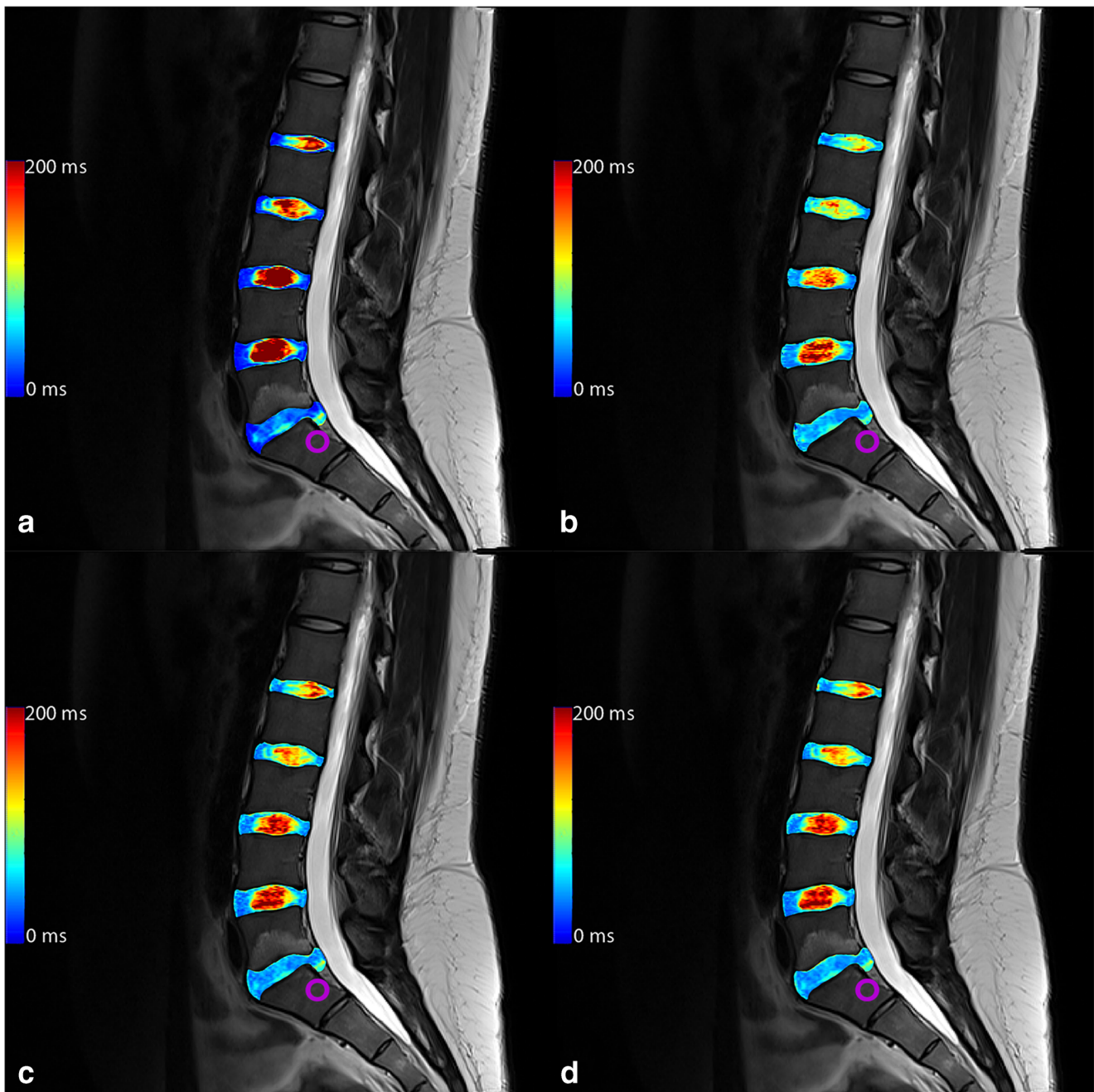


**Fig. 2** Color-coded  $T_2$  map overlays of (a) multi-echo spin-echo (MESE), (b) GRAPPATINI, (c) EVEN, and (d) WO1ST. The purple circle marks a herniating L5/S1 disc with annular tear with nucleus

pulposus tissue in the lower posterior annular region of interest, resulting in higher, pathological  $T_2$  at that very place and a consecutive acute bone marrow edema in L5

However, even after multiple promising studies,  $T_2$  mapping of hardly any cartilaginous tissue has found its way into clinical routine mainly due to the clinically unfeasible measurement times.

Our data confirm the aforementioned literature with significant differences of  $T_2$  values between the different grades of disc degeneration. However, GRAPPATINI was acquired in just 02:28 min with preserved spatial resolution. Furthermore, no sequence-specific artifacts were observed that would

impede assessment of an intervertebral disc. This facilitates  $T_2$  mapping of the entire lumbar spine in 02:28 min as opposed to 13:18 min using a conventional MESE sequence with the same sequence parameters.

Lumbar disc herniation is commonly found in the general population and frequently asymptomatic. However, the presence of lumbar disc herniation is an important finding in symptomatic patients as it significantly worsens prognosis [25]. Hoppe et al have already shown that  $T_2$  values significantly

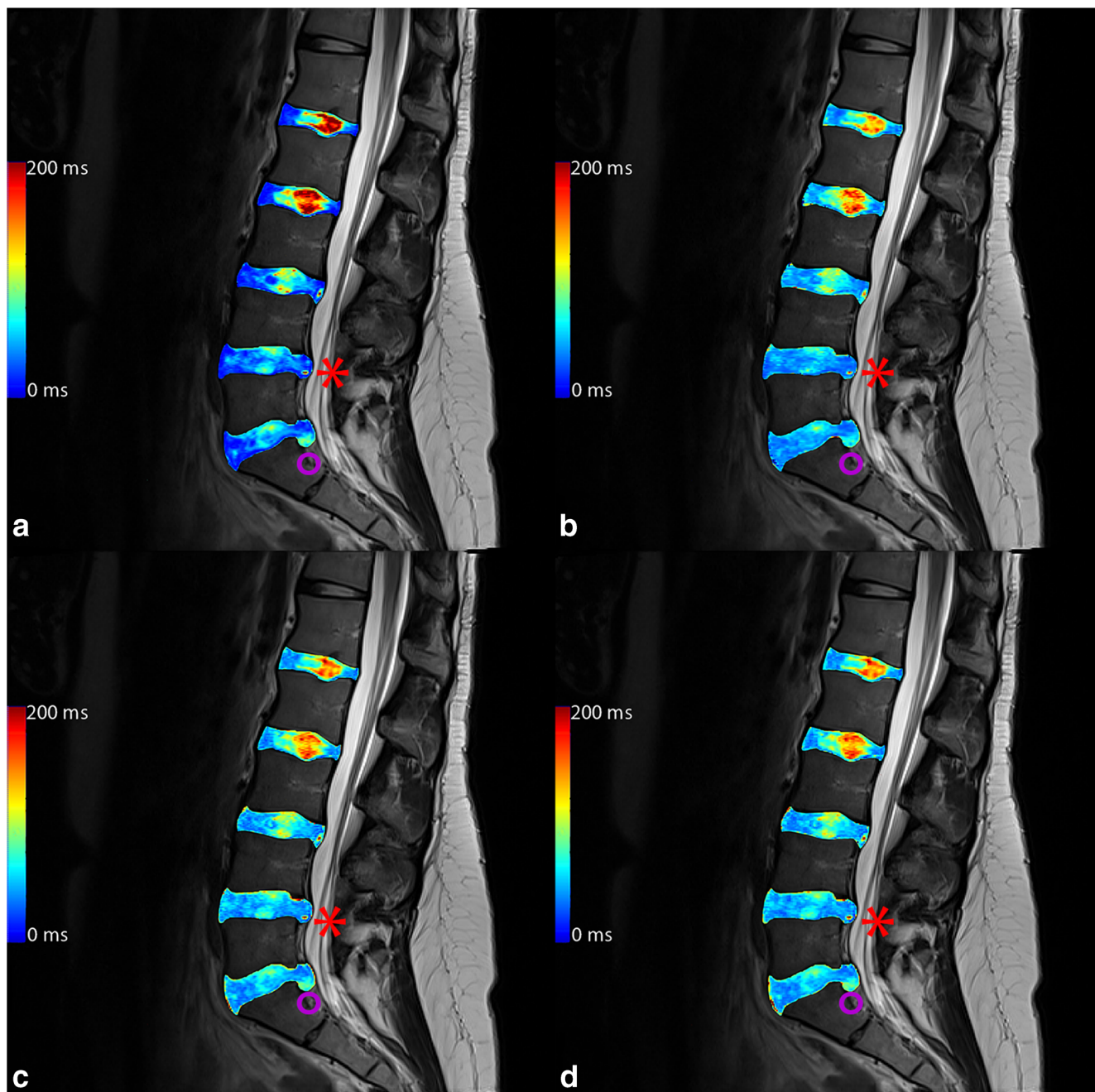


**Fig. 3** Color-coded  $T_2$  map overlays of **a** multi-echo spin-echo (MESE), **b** GRAPPATINI, **c** EVEN, and **d** WO1ST. The red asterisk marks a high-intensity zone in L4/L5 which can be clearly seen in all measurements (another small one tear can be seen on L3/L4 also). The purple circle

marks a herniating L5/S1 disc with annular tear with nucleus pulposus tissue in the lower posterior annular region of interest, resulting in higher, pathological  $T_2$  at that very place

differ between herniated and non-herniated discs [26]. In a 5-year follow-up study, the baseline  $T_2$  values of the nucleus pulposus could be used as a predictive biomarker for new lumbar disc herniation at follow-up [27].

Our data are coherent with the literature with significant  $T_2$  differences in normal discs compared to herniated discs with a similar performance for the investigated  $T_2$  mapping techniques as measured by the AUCs of calculated ROCs. However,  $T_{2-GRAPPATINI}$  was the only assessment showing

significant differences in the posterior annular region of herniated compared to normal discs.

Another important finding in general morphological imaging of the lumbar IVDs is the high-intensity zones of the posterior annulus fibrosus [17].

They are caused by torn fibro-cartilage lamellae of the annulus fibrosus containing trapped nucleus pulposus tissue. This promotes the ingrowth of vascularized granulation tissue into the disc. Simultaneously, sinuvertebral nerve endings



begin to sprout into the disc which attribute to the visceral pain qualities of chronic low back pain [4].

In this study, discs with HIZ showed significantly different  $T_2$  values in the nucleus pulposus and the posterior annular region compared to discs without HIZs with  $T_{2-GRAPPATINI}$  of the nucleus pulposus showing an AUC comparable to the other  $T_2$  mapping methods when testing for discriminability.

This is concordant with the findings of other studies that reported measurable differences in discs with and without HIZ using  $T_2$  mapping [28].

However, groups like Sharma et al have stated that annular tears precede and accelerate—or actually cause—disc degeneration rather than mainly occurring in already degenerated discs [29]. Our data suggest the contrary, hinting more at annular tear occurring earlier than the associated disc degeneration, as this study's participants were very young. However, this has to be proven by larger prospective or longitudinal case-control studies, which could be facilitated by accelerated  $T_2$  mapping sequences like GRAPPATINI.

Another noteworthy finding in the presented data is the significantly higher  $T_{2-MESE}$  of the nucleus pulposus when compared to  $T_{2-GRAPPATINI}$ ,  $T_{2-EVEN}$ , and  $T_{2-WO1ST}$ . This overestimation is mainly caused by stimulated echoes which instigate an increased signal proportion along the echo train. This results in an overestimated  $T_2$  relaxation time and unstable fitting procedure. The fitting can, however, be substantially improved by calculating the  $T_2$  maps without the first or with only even echoes, as reflected in  $T_{2-WO1ST}$  and  $T_{2-EVEN}$ . This approach to mitigate bias caused by stimulated echoes has already been used in other studies [14, 16], however still results in a small systemic overestimation of  $T_2$ .

Additionally, robust  $T_2$  mapping has been a challenging field for many years already due to imperfect slice profiles, field inhomogeneities, and flip angle offsets [30].

There are other attempts to shorten the acquisition time needed for  $T_2$  relaxation time measurements, like radial  $T_2$  mapping sequences, the three-dimensional triple-echo steady-state sequence, or, in a much broader perspective, magnetic resonance fingerprinting (MRF) [31–33]. However, none of the aforementioned has been effectively used in  $T_2$  mapping of the lumbar intervertebral disc to this date. This can be attributed mostly to the heterogeneity in the field of view, significant pulsation artifacts from the aorta, and the challenging distance combined with the narrow potential for parallel imaging using spine coils [32].

Also, MRF remains a promising, but investigational approach with ongoing dispute considering the generation of used dictionaries, image reconstructions requiring unusual computational resources, and the currently restricted in-plane resolution in clinically feasible acquisition times.

This study has some limitations to be addressed.

First, GRAPPATINI requires a long echo train since it uses the information along the echoes to recover non-sampled k-space lines. Consequently, the final protocol had to include 16 echoes ( $TE_{max} = 144$  ms) for an undersampling factor of 5, which may cause the fitting of a noise plateau in the calculated  $T_2$  decay for voxels with shorter relaxation times. However, this can be relativized by the annular  $T_2$  values which still show significant differences for the assessed pathologies at relatively short  $T_2$  times which were not superimposed by a noise component.

Also, the studied individuals of this study were comparably young. This, however, was intended, as the idea was to assess early stages of degeneration and pathology. In the end, there were enough cases of already degenerated or herniated discs to allow for a sufficient analysis.

Additionally, the segmentation used for the  $T_2$  value assessment was done by one single reader who was blinded to any clinical information. The segmentation was, however, copied from the  $T_2w$  TSE images to the resampled  $T_2$  maps, so there was no observer-based difference in the respective quantitative sequence comparisons.

In conclusion, the presented study shows that “generalized autocalibrating partially parallel acquisition and model-based accelerated relaxometry by iterative non-linear inversion,” in short GRAPPATINI, facilitates robust  $T_2$  mapping with a ten-fold reduction of measurement time (2:27 min) with the potential to use the resulting  $T_2$  maps as an imaging biomarker for disc degeneration, annular tear, and herniation. At the same time,  $T_{2-GRAPPATINI}$  showed an equal or better performance when directly compared to  $T_{2-MESE}$ ,  $T_{2-EVEN}$ , and  $T_{2-WO1ST}$ .

**Funding** Open access funding provided by Austrian Science Fund (FWF). This study has received funding from the Austrian Science Fund (TRP-L194-B05 and KLI541-B30).

## Compliance with ethical standards

**Guarantor** The scientific guarantor of this publication is Prof. Siegfried Trattnig, MD.

**Conflict of interest** The authors of this manuscript declare relationships with the following companies: Tom Hilbert and Tobias Kober are employees of Siemens Healthcare (Erlangen, Germany).

**Statistics and biometry** One of the authors (Michael Weber) has significant statistical expertise.

**Informed consent** Written informed consent was obtained from all subjects (patients) in this study.

**Ethical approval** Institutional Review Board approval was obtained.

**Study subjects or cohorts overlap** Some study subjects or cohorts have been previously reported in a not yet published paper accepted by *Investigative Radiology*. However, none of the statistical examinations

overlaps as the submitted manuscript is the first one to assess GRAPPATINI's synthetic T<sub>2</sub>-weighted images.

#### Methodology

- prospective
- cross-sectional study—observational
- performed at one institution

**Open Access** This article is licensed under a Creative Commons Attribution 4.0 International License, which permits use, sharing, adaptation, distribution and reproduction in any medium or format, as long as you give appropriate credit to the original author(s) and the source, provide a link to the Creative Commons licence, and indicate if changes were made. The images or other third party material in this article are included in the article's Creative Commons licence, unless indicated otherwise in a credit line to the material. If material is not included in the article's Creative Commons licence and your intended use is not permitted by statutory regulation or exceeds the permitted use, you will need to obtain permission directly from the copyright holder. To view a copy of this licence, visit <http://creativecommons.org/licenses/by/4.0/>.

## References

- GBD 2016 Disease and Injury Incidence and Prevalence Collaborators (2017) Global, regional, and national incidence, prevalence, and years lived with disability for 328 diseases and injuries for 195 countries, 1990–2016: a systematic analysis for the Global Burden of Disease Study 2016. *Lancet* 390:1211–1259
- Antoniou J, Steffen T, Nelson F et al (1996) The human lumbar intervertebral disc: evidence for changes in the biosynthesis and denaturation of the extracellular matrix with growth, maturation, ageing, and degeneration. *J Clin Invest* 98:996–1003
- Adams MA, Roughley PJ (2006) What is intervertebral disc degeneration, and what causes it? *Spine (Phila Pa 1976)* 31:2151–2161
- Rea W, Kapur S, Mutagi H (2012) Intervertebral disc as a source of pain. *Contin Educ Anaesth Crit Care Pain* 12:279–282
- Modic MT, Ross JS (2007) Lumbar degenerative disk disease. *Radiology* 245:43–61
- Pfirrmann CW, Metzendorf A, Zanetti M, Hodler J, Boos N (2001) Magnetic resonance classification of lumbar intervertebral disc degeneration. *Spine (Phila Pa 1976)* 26:1873–1878
- Stelzeneder D, Welsch GH, Kovacs BK et al (2012) Quantitative T2 evaluation at 3.0T compared to morphological grading of the lumbar intervertebral disc: a standardized evaluation approach in patients with low back pain. *Eur J Radiol* 81:324–330
- Ogon I, Takebayashi T, Takashima H et al (2015) Analysis of chronic low back pain with magnetic resonance imaging T2 mapping of lumbar intervertebral disc. *J Orthop Sci* 20:295–301
- Watanabe A, Benneker LM, Boesch C, Watanabe T, Obata T, Anderson SE (2007) Classification of intervertebral disk degeneration with axial T2 mapping. *AJR Am J Roentgenol* 189:936–942
- Blumenkrantz G, Zuo J, Li X, Kornak J, Link TM, Majumdar S (2010) In vivo 3.0-tesla magnetic resonance T1rho and T2 relaxation mapping in subjects with intervertebral disc degeneration and clinical symptoms. *Magn Reson Med* 63:1193–1200
- Marinelli NL, Haughton VM, Munoz A, Anderson PA (2009) T2 relaxation times of intervertebral disc tissue correlated with water content and proteoglycan content. *Spine (Phila Pa 1976)* 34:520–524
- Carr HY, Purcell EM (1954) Effects of diffusion on free precession in nuclear magnetic resonance experiments. *Phys Rev* 94:630–638
- Maier CF, Tan SG, Hariharan H, Potter HG (2003) T2 quantitation of articular cartilage at 1.5 T. *J Magn Reson Imaging* 17:358–364
- Hilbert T, Sumpf TJ, Weiland E et al (2018) Accelerated T2 mapping combining parallel MRI and model-based reconstruction: GRAPPATINI. *J Magn Reson Imaging* 48:359–368
- Galley J, Maestretti G, Koch G, Hoogewoud HM (2017) Real T1 relaxation time measurement and diurnal variation analysis of intervertebral discs in a healthy population of 50 volunteers. *Eur J Radiol* 87:13–19
- McPhee KC, Wilman AH (2018) Limitations of skipping echoes for exponential T2 fitting. *J Magn Reson Imaging* 48:1432–1440
- Fardon DF, Williams AL, Dohring EJ, Murtagh FR, Gabriel Rothman SL, Sze GK (2014) Lumbar disc nomenclature: version 2.0: recommendations of the combined task forces of the North American Spine Society, the American Society of Spine Radiology and the American Society of Neuroradiology. *Spine J* 14:2525–2545
- Yushkevich PA, Piven J, Hazlett HC et al (2006) User-guided 3D active contour segmentation of anatomical structures: significantly improved efficiency and reliability. *Neuroimage* 31:1116–1128
- Klein S, Staring M, Murphy K, Viergever MA, Pluim JP (2010) Elastix: a toolbox for intensity-based medical image registration. *IEEE Trans Med Imaging* 29:196–205
- Li G, Taljaard M, Van den Heuvel ER et al (2017) An introduction to multiplicity issues in clinical trials: the what, why, when and how. *Int J Epidemiol* 46:746–755
- Perry J, Haughton V, Anderson PA, Wu Y, Fine J, Mistretta C (2006) The value of T2 relaxation times to characterize lumbar intervertebral disks: preliminary results. *AJNR Am J Neuroradiol* 27:337–342
- Roberts S, Evans H, Trivedi J, Menage J (2006) Histology and pathology of the human intervertebral disc. *J Bone Joint Surg Am* 88(Suppl 2):10–14
- Trattning S, Stelzeneder D, Goed S et al (2010) Lumbar intervertebral disc abnormalities: comparison of quantitative T2 mapping with conventional MR at 3.0 T. *Eur Radiol* 20:2715–2722
- Schultz DS, Rodriguez AG, Hansma PK, Lotz JC (2009) Mechanical profiling of intervertebral discs. *J Biomech* 42:1154–1157
- Deyo RA, Mirza SK (2016) CLINICAL PRACTICE. Herniated lumbar intervertebral disk. *N Engl J Med* 374:1763–1772
- Hoppe S, Quirbach S, Mamisch TC, Krause FG, Werlen S, Benneker LM (2012) Axial T2 mapping in intervertebral discs: a new technique for assessment of intervertebral disc degeneration. *Eur Radiol* 22:2013–2019
- Raudner M, Schreiner MM, Juras V et al (2019) Prediction of lumbar disk herniation and clinical outcome using quantitative magnetic resonance imaging: a 5-year follow-up study. *Invest Radiol* 54:183–189
- Waldenberg C, Hebelka H, Brisby H, Lagerstrand KM (2019) Differences in IVD characteristics between low back pain patients and controls associated with HIZ as revealed with quantitative MRI. *PLoS One* 14:e0220952
- Sharma A, Pilgram T, Wippold FJ 2nd (2009) Association between annular tears and disk degeneration: a longitudinal study. *AJNR Am J Neuroradiol* 30:500–506
- Prasloski T, Madler B, Xiang QS, MacKay A, Jones C (2012) Applications of stimulated echo correction to multicomponent T2 analysis. *Magn Reson Med* 67:1803–1814
- Ben-Eliezer N, Sodickson DK, Shepherd T, Wiggins GC, Block KT (2016) Accelerated and motion-robust in vivo T2 mapping from radially undersampled data using block-simulation-based iterative reconstruction. *Magn Reson Med* 75:1346–1354
- Heule R, Ganter C, Bieri O (2014) Triple echo steady-state (TESS) relaxometry. *Magn Reson Med* 71:230–237
- Ma D, Gulani V, Seiberlich N et al (2013) Magnetic resonance fingerprinting. *Nature* 495:187–192

**Publisher's note** Springer Nature remains neutral with regard to jurisdictional claims in published maps and institutional affiliations.